

1 **Decoding the role of transcriptomic clocks in the human prefrontal cortex**

2 José J. Martínez-Magaña^{1,2}, John H. Krystal^{1,2,3}, Matthew J. Girgenti^{1,2}, Diana L. Núñez-
3 Ríos^{1,2}, Sheila T. Nagamatsu^{1,2}, Diego E. Andrade-Brito^{1,2}, Traumatic Stress Brain Research
4 Group, Janitza L. Montalvo-Ortiz^{1,2,3,*}

5 1 Division of Human Genetics, Department of Psychiatry, Yale University School of
6 Medicine, New Haven

7 2 National Center for PTSD, US Department of Veterans Affairs, West Haven, CT, USA

8 3 Psychiatry Service, VA Connecticut Health Care System, West Haven, CT, USA.

9

10 *Correspondence: Janitza L. Montalvo-Ortiz. Division of Human Genetics, Department of
11 Psychiatry, Yale University School of Medicine, New Haven. West Haven, CT, USA. Errera
12 Community Care Center-Orange Annex, 200 Edison Road, Office #1339, Orange, CT
13 06477. Email: janitza.montalvo-ortiz@yale.edu

14

15

16

17

18

19

20

21

22

23

24

25

26

27

28 **Abstract**

29 Aging is a complex process with interindividual variability, which can be measured by aging
30 biological clocks. Aging clocks are machine-learning algorithms guided by biological
31 information and associated with mortality risk and a wide range of health outcomes. One of
32 these aging clocks are transcriptomic clocks, which uses gene expression data to predict
33 biological age; however, their functional role is unknown. Here, we profiled two
34 transcriptomic clocks (RNAAgeCalc and knowledge-based deep neural network clock) in a
35 large dataset of human postmortem prefrontal cortex (PFC) samples. We identified that
36 deep-learning transcriptomic clock outperforms RNAAgeCalc to predict transcriptomic age in
37 the human PFC. We identified associations of transcriptomic clocks with psychiatric-related
38 traits. Further, we applied system biology algorithms to identify common gene networks
39 among both clocks and performed pathways enrichment analyses to assess its functionality
40 and prioritize genes involved in the aging processes. Identified gene networks showed
41 enrichment for diseases of signal transduction by growth factor receptors and second
42 messenger pathways. We also observed enrichment of genome-wide signals of mental and
43 physical health outcomes and identified genes previously associated with human brain
44 aging. Our findings suggest a link between transcriptomic aging and health disorders,
45 including psychiatric traits. Further, it reveals functional genes within the human PFC that
46 may play an important role in aging and health risk.

47 **Keywords:** Biological clocks, aging, prefrontal cortex, transcriptomic clocks, deep learning

48
49
50
51
52
53
54
55

56 **Main**

57 Aging is a complex biological process that can manifest differently and at a different rate in
58 each individual¹⁻³. The individual variability in biological aging can be measured, resulting in
59 the development of aging clocks⁴⁻⁶. Aging clocks are an excellent predictor of mortality and
60 lifespan⁷⁻¹⁰, as well as disease risk^{11,12}. One of the best-known aging clocks are epigenetic
61 clocks^{13,14}, which are based on age-related alterations in DNA methylation at CpG sites. We
62 and others have found a link between epigenetic clocks and psychiatric disorders¹⁵⁻¹⁸. Age-
63 associated biological changes can also occur at the RNA level^{19,20}. Recent studies of
64 transcriptomic clocks^{21,22} have shown associations with age-related disorders²⁰. These
65 clocks have been generated using several mathematical models, including the elastic net
66 model. However, such method is limited to a fixed set of genes for predicting age. Recently
67 developed deep learning methods can overcome this limitation²² by using the whole
68 transcriptome to train a neural network to select the most precisely defined and informative
69 set of genes.

70

71 The human prefrontal cortex (PFC) and other brain regions undergo molecular, structural,
72 and functional changes during aging²³⁻²⁵. Structural age-related alterations in the PFC in
73 older individuals are well-established by neuroimaging studies²⁶⁻³². A meta-analysis of 3,880
74 individuals showed that older people have a reduction in the activation of subcortical and
75 cortical brain regions compared with young adults measured by functional magnetic
76 resonance during a cognitive task³³. Molecular studies evaluating brain aging have found
77 that the PFC could age faster than other brain regions. For example, increased epigenetic
78 age in the PFC is observed compared to the cerebellum^{34,35}. Further, accelerated epigenetic
79 age in peripheral tissue has been associated with reduced cortical thickness^{36,37}. Recent work in
80 aging clocks have shown that those trained in peripheral tissues do not have the same
81 accuracy as those from the brain³⁸, with brain-trained clocks having a better chronological
82 age prediction accuracy³⁹. While some work has evaluated epigenetic clocks in the brain,
83 very few studies have examined transcriptomic clocks. Evaluating transcriptomic clocks is

84 important given recent evidence showing age-associated transcriptomic changes in the PFC
85 involving, for example, gene dysregulation of synaptic genes^{40–44}.

86

87 The present study aimed to profile a transcriptomic clock and to characterize its functional
88 impact in four human PFC regions (**Fig. 1**) from a large cohort of 551 human postmortem
89 brain samples. We highlight the advantage of deep learning methods to improve accuracy in
90 predicting brain transcriptomic age and identify that both clocks have concordance at
91 advanced ages. We replicated an association of the RNAAgeCalc with PTSD. Further, we
92 comprehensively characterized co-expressed genes shared by both clocks and prioritized
93 genes that could have an important role in aging within the human prefrontal cortex.

94

95 **Results**

96

97 ***Transcriptomic clocks performance in predicting age***

98 To estimate the transcriptomic age, we used two machine learning-based transcriptomic
99 clocks, the RNAAgeCalc²¹ and a clock that uses knowledge-primed artificial neural networks
100²². The RNAAgeCalc clock is a model that predicts tissue-specific transcriptomic age based
101 on a fixed set of coefficients for the genes calculated from a pre-trained elastic net model. In
102 this analysis, we used the model trained in brain tissue. The knowledge-primed artificial
103 neural network clock (neural clock) is a model that uses the RNAseq data as input and The
104 Molecular Signatures Database (MSigDB) hallmark gene set collection⁴⁵ to train a neural
105 network and estimate the transcriptomic age. A neural network is divided into layers; each
106 layer has several nodes, and each of these nodes inside a layer is called a neuron. The
107 neuron is relevant to predict the outcome, commonly named activation, if the statistical
108 model associates the neuron with the outcome. Based on the activation of each neuron in
109 the neural network, the model selects a different set of genes as predictors of chronological
110 age. Both transcriptomic clocks showed high correlations with chronological age. The neural
111 clock ($r = 0.89$, $p = 1.89e-56$) showed a higher correlation with chronological age compared

112 to the RNAAgeCalc ($r = 0.68$, $p = 3.34e-23$) (**Fig. 2A**) (**Supplementary Table 1A**). The
113 clocks also correlated between each other ($r = 0.65$, $p = 2.81e-20$) (**Fig. 2B**). The error in
114 age estimation was higher in the RNAAgeCalc (RMSE = 9.09 years) than in the neural clock
115 (RMSE = 5.55 years). Our results suggest that the deep learning clock showed better
116 accuracy in predicting age than RNAAgeCalc.

117

118 The estimations of delta-Age were higher in the RNAAgeCalc (**Fig. 2C**, **Supplementary**
119 **Table 1B**). Of the total PFC samples included in the testing set ($n = 160$), 65% ($n = 104$)
120 have a concordant delta-Age among both transcriptomic clocks (**Supplementary Table 1C**).
121 We also analyzed the distribution density of the transcriptomic age based on their discordant
122 or concordant effect (increased or decreased) on both clocks (**Fig. 2D - 2E**). We found that
123 the density of samples with a concordant decreased delta-Age clustered in advanced ages
124 for both clocks. We also found that samples showing concordant increased transcriptomic
125 age clustered at lower ages, whereas samples showing discordant effects did not show a
126 clustering pattern. These results suggest that transcriptomic clocks have the same prediction
127 accuracy at advanced chronological age, but this prediction accuracy could differ at lower
128 ages. Further, to evaluate if the transcriptomic age could also be correlated with advanced
129 age, we examined the correlation of the transcriptomic age with age and age squared. In the
130 correlation analysis with age squared, we found that the age squared was significant for both
131 clocks (**Supplementary Table 2**). This correlation suggests that the association of
132 transcriptomic age is not linear with chronological age at older age.

133

134 ***Associations of transcriptomic age with psychiatric-related phenotypes and potential*** 135 ***confounding covariates.***

136 We analyzed the relationship between transcriptomic age derived from two approaches and
137 psychiatric-related traits, including major depressive disorder, post-traumatic stress disorder,
138 opioid use, alcohol use, tobacco use, amphetamine use, cocaine use, and cause of death
139 and possible confounding variables (PMI, RIN, sex, PFC region, and relative cell-type

140 proportions). First, a multivariate regression analysis was performed followed by a stepwise
141 multivariate regression analysis to refine the variables associated with transcriptomic age. In
142 the multivariate model, we identified multiple associations with each transcriptomic clock
143 (**Supplementary Tables 3A - 4B**). The transcriptomic age estimated with the neural clock
144 was associated with neurons and endothelial cells, relative cell proportion. The RNAAgeCalc
145 transcriptomic age was associated with the OFC and sgPFC. In the stepwise multivariate
146 regression analysis, we identified associations between the Neural clock transcriptomic age
147 and opioid misuse and endothelial cells. In contrast, the RNAAgeCalc was associated with
148 posttraumatic stress disorder (PTSD), orbitofrontal cortex (OFC), and subgenual prefrontal
149 cortex (sgPFC). Concordant associations in both clocks include a negative association with
150 cause of death by overdose and relative neuron proportions (positively associated with
151 RNAAgeCalc and negatively associated with the neural clock). Overall, these results suggest
152 that the clocks have differential associations with psychiatric traits.

153

154 We also modelled an age squared term in the regression models to account for the effect of
155 increased chronological age in the transcriptomic age. When considering age squared in the
156 model, the age squared term was significant in both clocks (**Supplementary Table 5A - 6B**).
157 In the stepwise correlation analysis, age, age-squared, and neurons remained significant in
158 the Neural clock (**Fig. 2E**), whereas age, age squared, OFC, sgPFC, neurons, and COD
159 overdose remained significant in the RNAAgeCalc. Some of the associations found
160 previously were not replicated when adding the age squared term into the regression
161 models, suggesting that the effect of these traits in the transcriptomic age could not be the
162 same at different chronological ages and considering this variable in the analysis of the PFC
163 transcriptomic age could be important to model aging of the human PFC.

164

165 ***In silico functional analysis of the genes in the transcriptomic clocks***

166 To investigate potential functional implications of the transcriptomic clocks, we conducted
167 the following analyses: 1) functional enrichment analysis, 2) comparison with a cortical

168 epigenetic clock, and 3) associations with aging phenotypes. The genes used in the
169 RNAAgeCalc and neural clock models differed. These differences rely on the mathematical
170 modeling of the clocks. The RNAAgeCalc uses a fixed number of genes ($n = 1616$,
171 **Supplementary Table 7**) selected for the association with age, prioritizing each gene by an
172 elastic net algorithm ²¹. The knowledge-primed artificial neural network clock is based on a
173 deep neural network. In this clock, deep neural networks are built by layers where only some
174 layers are activated by the statistical model, to predict an outcome, chronological age. In this
175 clock, each layer is represented by each of the biological pathways in the MSigDB database,
176 building a compartmentalized network. The deep neural clock splits the genes of the
177 transcriptome into each biological pathway, and a gene predicted chronological age if all the
178 genes in this biological pathway are associated with chronological age. This clock selects
179 the best predictors for chronological age in the dataset; in this analysis, the neural clock
180 selected 4325 genes ²². Both clocks showed an overlap of 390 genes (7%).

181

182 Considering that the genes associated with both clocks could have a greater functional
183 impact on aging-related processes, we performed functional enrichment analysis. By using
184 Metascape, overlapped genes showed enrichment for 976 ontology and pathways
185 (**Supplementary Table 8**). The top enriched ontology/pathways, included diseases of signal
186 transduction by growth factor receptors and second messengers (R-HSA-5663202, ngenes
187 = 45), Epstein-Barr virus infection (hsa05169, ngenes = 27), ribonucleotide metabolic
188 process (GO:0009259, ngenes = 33), Pathways in cancer (hsa05200, ngenes = 36), and
189 cellular response to cytokine stimulus (GO:0071345, ngenes = 40) (**Fig. 3A**). When
190 evaluating previous genome-wide association signals, we identified enrichment in 45
191 disorders, with diastolic blood pressure, Crohn's disease, mean corpuscular hemoglobin,
192 and coronary artery disease (**Supplementary Table 9, Fig. 3B**) as top associations.
193 Enrichment for mental disorders was also observed, including schizophrenia (ngenes = 26,
194 q -value = $6.84e-04$), bipolar disorder (ngenes = 20, q -value = $3.47e-03$), and autism
195 spectrum disorder or schizophrenia (ngenes = 20, q -value = $9.88e-03$). Overall, these results

196 suggest that the overlapped genes could impact several biological pathways and are
197 associated with aging phenotypes, as well as other health-related traits, including psychiatric
198 traits.

199

200 Epigenetic clocks are the most commonly studied biological clocks and they are good
201 predictors of mortality and health outcomes. We analyzed whether genes of a cortical
202 epigenetic clock trained in the human PFC tissue ³⁸ overlapped with the genes of the
203 transcriptomic clocks (**Fig. 3C**). We found six genes overlapping among the three clocks
204 (*POU2F1*, *HLA-C*, *FGF17*, *PVT1*, *ADM*, and *ENO2*). When comparing each transcriptomic
205 clock with the cortical epigenetic clock (**Supplementary Table 10**), we found that the neural
206 clock showed a higher gene overlap (1.20%, ngenes = 72) with the epigenetic clock
207 compared to the RNAAgeCalc (0.20%, ngenes = 10, *RNPC3*, *GOSR1*, *ZNF518B*, *HSF4*,
208 *TATDN1*, *TATDN3*, *HLA-H*, *POLR1A*, *NUP62*, and *SSBP4*). The 72 overlapped genes
209 between the neural clock and the epigenetic clock were enriched in 20 ontologies and
210 pathways (**Supplementary Table 10**), with the most significant enrichment including the
211 Nuclear receptors meta-pathway (ngenes = 11) and enzyme-linked receptor protein
212 signaling pathway (ngenes = 12) (**Supplementary Table 11**). In the protein-protein
213 clustering of these 72 genes, performed by Metascape, we identified one gene cluster
214 containing the *HSPA1A*, *HSPA1L*, *CREBBP*, *POLR2A*, *CCND1*, and *CDKN1A* genes (**Fig.**
215 **3D**). We evaluated if the genes in both clocks could be regulated by a common transcription
216 factor by enrichment analysis. In the transcription factor enrichment analysis, we identified
217 55 factors that could target these overlapped genes; the most significant was the *BANP*
218 (**Supplementary Table 12**). We then evaluated the HAGR database ⁴⁶ to identify if any of
219 these transcription factors have been associated with aging phenotypes and, consequently,
220 acting as a regulatory gene in aging processes. We identified *FOXO4*, *E2F1*, *CEBPB*, and
221 *NRF2* with previous associations with aging phenotypes.

222

223 **Cell-type enrichment analysis**

224 To understand the cellular diversity associated with each transcriptomic clock, we conducted
225 the Expression Weighted Cell Type Enrichment (EWCE). In the Neural trained clock, we
226 identified enrichment for almost all cells at annotation level 1 (pyramidal CA1, pyramidal SS,
227 astrocytes ependymal, oligodendrocytes, endothelial mural, and microglia) (**Fig. 3E**,
228 **Supplementary Table 13A - B**). In contrast, RNAAgeCalc was enriched for the pyramidal
229 CA1, pyramidal SS, and endothelial mural cells (**Fig. 3E, Supplementary Table 13C - D**).
230 Thus, these cell-type enrichment analyses suggest that specific cell types differentially
231 contribute to different transcriptomic clocks.

232

233 ***Consensus network analysis***

234 Gene expression patterns can correlate among genes, and grouping highly correlated genes
235 in networks may identify genes with common biological functions. We used a system biology
236 approach to build a network of the overlapped genes between both clocks followed by
237 functional annotation. We identified 416 nodes and 4855 edges in the consensus network.
238 Of the 390 overlapped genes between both clocks, we identified that 192 genes (49.23%)
239 are co-expressed in all the brain PFC regions (**Supplementary Table 14**). These genes
240 were enriched in 358 ontologies and pathways (**Supplementary Table 15**). The five most
241 enriched pathways were Huntington disease (hsa05016, ngenes = 19), transport of small
242 molecules (R-HSA-382551, ngenes = 26), the citric acid (TCA) cycle/respiratory electron
243 transport (R-HSA-1428517, ngenes = 14), and membrane trafficking (R-HSA-199991,
244 ngenes = 23) (**Fig. 4A**). Also, of the 192 genes identified in the consensus network, we
245 found 71 in the HAGR database (**Supplementary Table 16**). This consensus network
246 showed a high enrichment of protein-protein interactions (PPI) (p-value < 1.00e-06). The PPI
247 network identified 55 genes clustered in 5 groups (**Fig. 4B**). Of the 55 genes identified in
248 these clusters, 5 (*XRCC6*, *YWHAZ*, *PRKAR2B*, *DLD*, and *YWHAG*) were identified in the
249 HAGR database. The genes of this consensus network were also enriched in 14
250 transcription factors, with *NRF2* as the most significant, a transcription factor also included in
251 the HAGR database (**Fig. 4C**). This consensus network that targets *NRF2* contains 16

252 genes (*ALDOA*, *ATP1B1*, *ATP6V0A1*, *DMD*, *HSP90AB1*, *PAFAH1B1*, *PFN2*, *PSMD12*,
253 *RAN*, *SKP1*, *TUBA4A*, *YWHAG*, *USP14*, *RTN3*, *CAB39*, and *TUBB*). The consensus
254 network analysis identified genes associated with the aging process and identified *NRF2* as
255 the potential transcription factor regulating the expression of genes common in both clocks.

256

257 We explored the enrichment of these highly conserved co-expressed genes in the synapsis
258 using SynGO. Enrichment of the consensus network was observed in the synapsis (**Fig. 4D**,
259 **Supplementary Table 17**), including the *EIF2S1*, *ARPC5L*, *RTN3*, *YWHAG*, *AP2M1*, *NAPA*,
260 *NAPB*, *PFN2*, *HSPA8*, *VPS35*, *ADD2*, *ARFGEF2*, *GAD1*, *PRKCE*, *NSF*, *GDI1*, *VDAC1*,
261 *ATP2B1*, *CLTC*, *DNM1L*, *ATP6V1E1*, *SCAMP1*, *MAL2*, *ATP6V0D1*, *ATP6V0A1*, *CNTN1*,
262 *KCNA4*, *ATP1A3*, *SCN2A*, *PRKAR2B*, *NCKAP1*, *ACTR2*, *YWHAZ*, *DMD*, *PAK3*, and *MAG*
263 genes. Of these 36 genes, six genes (*HSPA8*, *YWHAZ*, *PRKAR2B*, *DMD*, *GAD1*, and
264 *YWHAG*) were found in the HAGR database. This enrichment suggests that genes common
265 in both transcriptomic clocks have a role in synaptic processes.

266

267 **Discussion**

268 Here, we report a comprehensive study examining the role and functionality of transcriptomic
269 clocks in a large cohort of human postmortem PFC. Biological clocks, predominantly
270 epigenetic clocks, predict aspects of morbidity and mortality. We compared two different
271 transcriptomic clocks and found that while both can predict age, the knowledge-primed
272 artificial neural networks, trained with deep learning techniques, outperforms RNAAgeCalc.
273 The advantage of deep learning techniques in predicting age has been previously reported
274 for epigenetic clocks^{47,48}. However, even with the higher prediction accuracy, the neural
275 clock correlated with fewer phenotypes compared to the RNAAgeCalc. The observed
276 differences could be due to low gene overlap between the transcriptomic clocks driven by
277 distinct feature selection in each model. This is also observed in epigenetic clocks, where
278 multiple and different sets of CpG sites have been used to predict age, with some achieving
279 comparable accuracy⁴⁹.

280

281 Our stepwise multivariate analysis of RNAAgeCalc found that PTSD is associated with PFC
282 transcriptomic age. This association is consistent with previous findings from peripheral
283 blood and brain. For instance, a previous study using RNAAgeCalc identified an accelerated
284 transcriptional age in 324 World Trade Center responders⁵⁰. Further, an epigenetic age
285 acceleration in the motor cortex⁵¹ and transcriptomic age acceleration in the ventromedial
286 PFC has been reported in PTSD cases⁴⁴. These findings suggest that individuals diagnosed
287 with PTSD exhibit accelerated aging, reflected at both the transcriptomic and epigenomic
288 levels. We also found that the correlation with PTSD was not significant when including an
289 age-squared term in the model, suggesting that the effect of age in transcriptomic age is not
290 linear in the PFC, a phenomenon also observed in epigenetic clocks^{38,52}. A similar effect of
291 the age-squared was found in the correlation of the neural transcriptomic clock and opioid
292 misuse. We found an association of opioid misuse with advanced transcriptomic age, which
293 was not replicated when including the age-squared term in the regression model. This
294 deviation in age at advanced ages could be an effect of the training model. Another
295 explanation is that aging processes could be different at advanced ages compared to other
296 stages of the lifespan. For example, a previous study reported that the effect of body mass
297 index on epigenetic age was found only in young people but not in nonagenarians⁵³.
298 Estimating biological age in older ages is still underexplored; further studies are needed to
299 understand the differences of biological aging across the lifespan.

300

301 Our convergent analysis of transcriptomic and epigenetic cortical clocks identified six
302 overlapped genes between the three clocks. These genes are involved in blood-brain barrier
303 integrity and oligodendrocyte function. Among these genes, we found *ADM*
304 (adrenomedullin), a hypotensive peptide secreted by endothelial cells⁵⁴ and involved in
305 blood-brain barrier structure⁵⁵. *ADM* protein is also included in the recently developed
306 epigenetic clock GrimAge⁹, further supporting its role in aging. Even though the exact
307 mechanisms of *ADM* in aging are still unknown, recent animal studies suggest a role in

308 neurodegenerative diseases^{56,57}. Another convergent gene between the three clocks is
309 *FGF17* (fibroblast growth factor 17), implicated in oligodendrocyte function. Recently, a study
310 where aged mice were infused with cerebrospinal fluid from young mice found that *Fgf17*
311 regulates oligodendrogenesis in the hippocampus, which correlated with an improvement in
312 memory tasks⁵⁸.

313

314 Our consensus network analysis identified 192 co-expressed genes in the four PFC regions
315 shared by both clocks and enriched in synaptic processes, supporting a role of synaptic
316 changes in the PFC during aging⁵⁹. Further, we identified genes involved in mitochondria
317 functioning and dystrophic neurites. During the aging process, the mitochondria accumulate
318 a plethora of anomalies, promoting an accumulation of dysfunctional mitochondria, which
319 may lead to neuronal alterations and are suggested as common mechanisms for several
320 neurodegenerative diseases, such as Alzheimer's disease⁶⁰⁻⁶³. For example, in patients and
321 animal models of Alzheimer's disease, imbalance of mitochondrial dynamics⁶⁴, decreased
322 bioenergetics⁶⁵, and increased mitochondrial calcium levels are associated with neuronal
323 death⁶⁶. Besides, the functional analysis of the consensus network found that the
324 transcription factor *NRF2* (Nuclear factor erythroid 2-related factor 2) could be involved in
325 regulating the genes used to predict transcriptomic age. *NRF2* was enriched in the co-
326 expressed genes used as predictors in both clocks. This gene is considered a master
327 regulator of the cellular antioxidant defense system⁶⁷, controlling the expression of genes
328 with antioxidant response elements (ARE) in their promoters and activating genes with
329 cytoprotective activity⁶⁸⁻⁷¹. In addition, *NRF2* is upregulated in animal models with
330 exceptional longevity, like the mole-rat^{72,73}, and under caloric restriction, an intervention
331 reported to have an effect in increasing longevity in animal models⁷⁴⁻⁷⁸.

332

333 Overall, we conducted a comprehensive transcriptomic clock study of four PFC regions in a
334 large human postmortem brain cohort. Our findings suggest an association between PTSD

335 and transcriptomic aging. Further, we identified functional genes within the human PFC that
336 may play an important role in the aging process.

337

338 **Limitations**

339 In the analysis of the knowledge primed deep neural clock, we have to split the sample into a
340 training and testing set, thus reducing our sample size to perform associations with the
341 phenotypic traits. Still, our cohort is larger than similar to recent work ⁴⁴. Also, this reduction
342 in sample size did not allow us to stratify the sample by sex to potential sex-specific effects.

343

344 **Methods**

345

346 ***Sample population***

347 We included 551 human postmortem brain samples 143 individuals from the National Center
348 for PTSD Brain Bank ⁸⁰. Psychiatric history and demographic information were obtained by
349 psychological autopsies performed postmortem by next of kin. Diagnostic and Statistical
350 Manual of Mental Disorders version 4 (DSM-IV) criteria and the Structured Clinical Interview
351 for DSM-IV Axis I Disorders (SCID-1) interviews were adapted for psychological autopsy and
352 were used to define the diagnosis. All consents were acquired for the next of kin.

353

354 ***RNA Sequencing***

355 RNA from each brain region was extracted using the RNeasy Mini kit with genomic DNA
356 elimination, as described by the manufacturer (Qiagen). The RNA integrity number (RIN)
357 and concentration were assessed using a Bioanalyzer (Agilent). Libraries were constructed
358 using a SMARTer Stranded RNA-seq kit (Takara Bio). rRNA depletion was performed using
359 a Ribozero Gold kit (Illumina). Samples were paired-end sequenced on an Illumina
360 HiSeq4000 with a read length of 75 base pairs and targeting a depth of 50 million reads.
361 Sequences in the FASTQ files were mapped to the human genome using STAR (v.2.5.3a) ⁸¹

362 with the reference genome (release 79, GRCh38). We used RNA-SeQC⁸² to quantify the
363 transcripts using Ensembl's gene transfer format (GTF) annotation file.

364

365

366 ***Transcriptomic clocks analyses***

367 To estimate the transcriptomic age, we used two machine learning-based transcriptomic
368 clocks, the RNAAgeCalc²¹ and a clock that uses knowledge-primed artificial neural networks
369²². The RNAAgeCalc clock is a model that predicts the tissue-specific transcriptomic age
370 based on a fixed set of coefficients for the genes calculated from a pre-trained elastic net
371 model; in this analysis, we used the model trained in brain tissue. We used the *RNAAgeCalc*
372 R package R²¹ and used raw counts of the RNA sequencing analysis from all samples. The
373 knowledge-primed artificial neural network clock (neural clock) is a model that uses the
374 RNAseq data as input and The Molecular Signatures Database (MSigDB) hallmark gene set
375 collection⁴⁵ as input to train a neural network and estimate the transcriptomic age. Based on
376 the activation of each neuron in the neural network, the model selects a different set of
377 genes as predictors of chronological age. Conditional quantile normalization was conducted
378 using the *cqn* R package⁸³. For the neural clock analysis, we randomly split the postmortem
379 brain samples into training (2/3 of the brain samples) and testing datasets (1/3 of the brain
380 samples) (**Supplementary Table 18**).

381

382 ***Predictive age accuracy of transcriptomic clocks***

383 Since the neural clock uses the training dataset to estimate the set of genes that better
384 predicts the chronological age, we only used the testing dataset to explore the predictive
385 accuracy of the clocks. First, we performed pairwise Pearson correlations between the
386 chronological and transcriptomic age; and between the predicted biological ages from both
387 clocks. In addition, we estimated the prediction error of transcriptomic age using the root
388 mean square error (RMSE) measurement implemented in the *rmse* function of the *Metrics* R
389 package. We also calculated the delta of age (delta-Age) as the difference between

390 transcriptomic and chronological age ($\text{delta-Age} = \text{transcriptomic age} - \text{chronological age}$). If
391 the transcriptomic age is higher than the chronological age ($\text{delta-Age} > 0$), we classified the
392 sample as having an increased transcriptomic age (i.e, positive delta-Age). If the
393 transcriptomic age is lower than the chronological age ($\text{delta-Age} < 0$), we classified the
394 sample as decreased transcriptomic age (i.e, negative delta-Age). To estimate the
395 concordance (i.e, samples with increased transcriptomic age in both clocks) between the
396 delta-Age values of the transcriptomic clocks, we counted the number of samples that had
397 estimated concordance between both clocks and those that had discordant results in both
398 clocks (i.e, samples with increased transcriptomic age in one clock but decreased in the
399 other) and compared these counts by a chi-squared test. All analyses were performed in R
400 version 4.1.1⁸⁴.

401

402 ***Analysis of transcriptomic clocks with age***

403 To test associations between chronological age and transcriptomic age, we regressed
404 transcriptomic age against chronological age. By definition, transcriptomic age is correlated
405 with chronological age, but if it varies non-linearly with chronological age, the estimations in
406 the older ages could be different. Therefore, we tested the extent to which the prediction
407 accuracy of the transcriptomic clocks correlates with age by including an age-squared term
408 in the regression model. All the correlations analyses were performed in R version 4.1.1⁸⁴.

409

410 ***Association of transcriptomic age acceleration with phenotypic traits***

411 To test the association of the transcriptomic clocks with multiple phenotypic traits, we tested
412 multivariable models in two ways: a complete model (a model including all the covariates in
413 the regression model) and a step-wise correlation model to identify the most predictive
414 variables. In this multivariable model, we regressed the transcriptomic age with age, sex,
415 major depressive disorder (MDD), posttraumatic stress disorder (PTSD), opioid misuse,
416 cause of death (classified as overdose, traumatic injury, or other causes of death), tobacco
417 use at the time of death, alcohol use at the time of death, amphetamine misuse, and cocaine

418 misuse. We combined all the brain regions for these models and added the brain region as a
419 covariate. We also included the model's postmortem interval (PMI), RNA integrity number
420 (RIN), and relative cell-type proportions as possible confounders. Relative cell-type
421 proportions were estimated using the Brain cell type-specific analysis implemented in the
422 *Brettigea* R package⁸⁵. For the step-wise correlation models, we used the *stepAIC* function
423 in the *MASS* package. We performed the regressions again using the same models,
424 multivariate and step-wise, but including an age-squared variable. The age-squared term
425 was included to verify if the association remained significant after adding the non-linear age
426 variable. All the correlations were analyzed in R⁸⁴.

427

428 ***Cell-type enrichment analysis***

429 To understand the cell-type diversity in each transcriptomic clock, we conducted the
430 Expression Weighted Cell Type Enrichment (EWCE) analysis and used the reported single-
431 cell transcriptome reference data. EWCE is a method that uses single-cell transcriptomes to
432 generate the probability distribution of a gene list having an average expression level within
433 different cell types⁸⁶. This analysis allows us to estimate the enrichment in two levels of cell
434 annotation depending on cell differentiation. For example, annotation level 1 would be
435 interneurons, and annotation level 2 would break this interneuron into 16 different
436 interneurons subtypes depending on your reference dataset.

437

438 ***Gene overlap with prefrontal cortex epigenetic clock***

439 To identify genes that overlap between transcriptomic and epigenetic clocks, we annotated
440 the 347 CpG sites of a previously published epigenetic clock³⁸, trained to predict epigenetic
441 age in the human prefrontal cortex, to their closest genes using the
442 *IlluminaHumanMethylationEPICanno.ilm10b2.hg19* package.

443

444 ***Construction of a consensus network (CoDiNA)***

445 Gene co-expression networks are useful for identifying a set of genes that could be
446 biologically relevant and could be coregulated^{87,88}. Most gene co-expression network
447 methods infer independent networks, which could generate inconsistencies in the network
448 construction. The construction of consensus networks has been recently proposed to
449 overcome this limitation⁸⁹. We used co-expression differential network analysis implemented
450 in the *CoDiNA* package⁹⁰ to identify a consensus network in the PFC regions. We built
451 independent networks for dACC, OFC, dlPFC, and sgPFC using the *wTO* package⁹¹ using
452 the common genes as predictors of age in both transcriptomic clocks. We used conditional
453 quantile normalized counts and extracted the co-expressed genes in the four PFC regions.

454

455 ***Functional analyses***

456 Functional analyses were conducted, including enrichment analysis and protein-protein
457 interaction (PPI) networks, by using Metascape⁹², a web-based portal that integrates a
458 broad set of current biological databases and applies analytical pipelines to perform a
459 comprehensive gene list annotation. Most of the known biological databases are redundant,
460 and reducing this redundancy is helpful to have more biological interpretable results.
461 Metascape applies a hierarchical clustering algorithm that reduces redundancies into
462 representative clusters. PPI analysis was performed to infer biologically interpretable results
463 from complex networks. For this, we used Metascape, which applies a mature complex
464 identification algorithm called Molecular Complex Detection (MCODE)⁹³ that detects densely
465 connected regions in PPI networks. Enrichment analyses were performed of the overlapped
466 genes in both transcriptomic clocks and those found in the consensus network.

467

468 ***Synopsis GO (SynGO) enrichment analysis***

469 Synaptic processes play a role in the brain aging process⁵⁹. To explore if the transcriptomic
470 clocks include genes with a synaptic function, we performed an enrichment analysis using
471 the GO synopsis database (SynGO)⁹⁴. We also performed a synopsis GO enrichment
472 analysis of the genes identified in the consensus network.

473

474 ***Human aging genomic resources (HAGR)***

475 To assess whether the genes in the transcriptomic clocks have been previously associated
476 with aging, we queried the Human aging genomic resource (HAGR) database ⁴⁶, an online
477 collection of multiple databases containing genes associated with aging.

478

479 **Acknowledgments**

480 We want to thank Dr. Lars Kaderali and Dr. Nicholas Holzschek for sharing the scripts to
481 model the knowledge-primmed artificial neural network clock. We also want to thank the
482 brain donors and their families thar made this research possible as well as the members of
483 the Traumatic Stress Brain Research Group: Victor E. Alvarez, MD; David Benedek, MD;
484 Alicia Che, PhD; Dianne A. Cruz, MS; David A. Davis, PhD; Ellen Hoffman, MD, PhD; Paul
485 E. Holtzheimer, MD; Bertrand R. Huber, MD, PhD; Alfred Kaye, MD, PhD; Adam T.
486 Labadorf, PhD; Terence M. Keane, PhD; Mark W. Logue, PhD; Ann McKee, MD; Brian
487 Marx, PhD; Deborah Mash, MD; Mark W. Miller, PhD; Crystal Noller, PhD; William K. Scott,
488 PhD; Paula Schnurr, PhD; Thor Stein, MD, PhD; Robert Ursano, MD; Douglas E.
489 Williamson, PhD; Erika J. Wolf, PhD, Keith A. Young, PhD. This work is supported by the
490 U.S. Department of Veterans Affairs via 1IK2CX002095-01A1 (JLMO), the National Center
491 for PTSD, and NIDA R21DA050160 (JLMO).

492

493 **Contributions**

494 JLMO and JJMM conceptualized the study. JJMM analyzed the data. JJMM and JLMO
495 wrote the original manuscript. JHK, DLNR, and STN contributed to the interpretation of the
496 results. JHK, MJG, DLNR, STN, and DEAB edited it. All authors revised the manuscript and
497 approved the final version.

498

499 **Conflict of interest**

500 No authors report a conflict of interest.

501

502 **Figure Legends**

503 **Fig. 1** Schematic study workflow. We performed RNAseq of 551 postmortem human
504 prefrontal cortex (PFC) brain samples from 143 individuals and estimated the transcriptomic
505 age using two aging clocks, RNAAgeCalc, and a knowledge-based deep neural network
506 clock (neural clock). Then, we correlated transcriptomic age with age and psychiatric
507 phenotypes and evaluated the prediction accuracy of both clocks. Further, we analyzed the
508 co-expression network shared between the four PFC regions and performed a functional
509 analysis with several databases and algorithms.

510 **Fig. 2** Correlations of transcriptomic age with several phenotypes. A) Correlation between
511 chronological age and transcriptomic age, the orange line represents the RNAAgeCalc and
512 blue the neural clock; B) Pairwise correlations between chronological age and the
513 transcriptomic clocks; C) Mean of the delta of age (dAge) in samples separated by
514 decreased and increased dAge. Blue represents the neural clock, and orange the
515 RNAAgeCalc; D) Density plots of the correlation between chronological and transcriptomic
516 age. Blue represents the density of the distribution of individuals with concordant increased
517 transcriptomic age, green represents samples with discordance between transcriptomic age,
518 red represents concordance with decreased age acceleration, and E) Effect sizes of the
519 most predictive features in the pairwise correlation.

520 **Fig. 3** Functional analysis and cell-type enrichment analysis of the overlap of both clocks. A)
521 Top 10 most significant gene ontologies and pathways after redundancy removal in the
522 clusters; B) Genome-wide enrichment analysis of the genes that overlap between both
523 clocks; C) Gene overlap between the genes used by the transcriptomic locks and the
524 epigenetic clock; D) MCODE of the protein-protein interaction network of the genes that
525 overlap between the neural clock and the epigenetic cortical clock; E) Cell-type enrichment
526 analysis of the genes in the neural clock (blue) and RNAAgeCalc (orange) at annotation
527 level 1.

528 **Fig. 4** Functional annotation of the consensus network. A) Top 10 enriched gene ontologies
529 and pathways after redundancy removal; B) MCODE clusters of the protein-protein
530 interaction network analysis; C) Transcription factor enrichment analysis of the consensus
531 network; and D) Synaptic enrichment analysis of the consensus network.

532

533 **References**

- 534 1. Niccoli, T. & Partridge, L. Ageing as a risk factor for disease. *Curr. Biol. CB* **22**, R741-
535 752 (2012).
- 536 2. López-Otín, C., Blasco, M. A., Partridge, L., Serrano, M. & Kroemer, G. The hallmarks
537 of aging. *Cell* **153**, 1194–1217 (2013).
- 538 3. Lemoine, M. The Evolution of the Hallmarks of Aging. *Front. Genet.* **12**, 693071 (2021).
- 539 4. Ferrucci, L. *et al.* Measuring biological aging in humans: A quest. *Aging Cell* **19**,
540 e13080 (2020).
- 541 5. Seale, K., Horvath, S., Teschendorff, A., Eynon, N. & Voisin, S. Making sense of the
542 ageing methylome. *Nat. Rev. Genet.* **23**, 585–605 (2022).
- 543 6. Rutledge, J., Oh, H. & Wyss-Coray, T. Measuring biological age using omics data. *Nat.*
544 *Rev. Genet.* (2022) doi:10.1038/s41576-022-00511-7.
- 545 7. Tanaka, T. *et al.* Plasma proteomic signature of age in healthy humans. *Aging Cell* **17**,
546 e12799 (2018).
- 547 8. Levine, M. E. *et al.* An epigenetic biomarker of aging for lifespan and healthspan. *Aging*
548 **10**, 573–591 (2018).
- 549 9. Lu, A. T. *et al.* DNA methylation GrimAge strongly predicts lifespan and healthspan.
550 *Aging* **11**, 303–327 (2019).
- 551 10. Belsky, D. W. *et al.* Quantification of the pace of biological aging in humans through a
552 blood test, the DunedinPoAm DNA methylation algorithm. *eLife* **9**, e54870 (2020).
- 553 11. Ling, C. & Rönn, T. Epigenetics in Human Obesity and Type 2 Diabetes. *Cell Metab.*
554 **29**, 1028–1044 (2019).
- 555 12. Herman, A. B., O’Connor, J. R. & Sen, P. Epigenetic dysregulation in cardiovascular

- 556 aging and disease. *J. Cardiovasc. Aging* **1**, 10 (2021).
- 557 13. Hannum, G. *et al.* Genome-wide methylation profiles reveal quantitative views of
558 human aging rates. *Mol. Cell* **49**, 359–367 (2013).
- 559 14. Horvath, S. DNA methylation age of human tissues and cell types. *Genome Biol.* **14**,
560 R115 (2013).
- 561 15. Tamman, A. J. F. *et al.* Accelerated DNA Methylation Aging in U.S. Military Veterans:
562 Results From the National Health and Resilience in Veterans Study. *Am. J. Geriatr.*
563 *Psychiatry Off. J. Am. Assoc. Geriatr. Psychiatry* **27**, 528–532 (2019).
- 564 16. Montalvo-Ortiz, J. L., Cheng, Z., Kranzler, H. R., Zhang, H. & Gelernter, J.
565 Genomewide Study of Epigenetic Biomarkers of Opioid Dependence in European-
566 American Women. *Sci. Rep.* **9**, 4660 (2019).
- 567 17. Okazaki, S. *et al.* Decelerated epigenetic aging associated with mood stabilizers in the
568 blood of patients with bipolar disorder. *Transl. Psychiatry* **10**, 129 (2020).
- 569 18. Chrusciel, J. H. *et al.* A systematic review and meta-analysis of epigenetic clocks in
570 schizophrenia. *Schizophr. Res.* **246**, 172–174 (2022).
- 571 19. van den Akker, E. B. *et al.* Meta-analysis on blood transcriptomic studies identifies
572 consistently coexpressed protein-protein interaction modules as robust markers of
573 human aging. *Aging Cell* **13**, 216–225 (2014).
- 574 20. Peters, M. J. *et al.* The transcriptional landscape of age in human peripheral blood. *Nat.*
575 *Commun.* **6**, 8570 (2015).
- 576 21. Ren, X. & Kuan, P. F. RNAAgeCalc: A multi-tissue transcriptional age calculator. *PLoS*
577 *One* **15**, e0237006 (2020).
- 578 22. Holzschek, N. *et al.* Modeling transcriptomic age using knowledge-primed artificial
579 neural networks. *NPJ Aging Mech. Dis.* **7**, 15 (2021).
- 580 23. Roberts, K. L. & Allen, H. A. Perception and Cognition in the Ageing Brain: A Brief
581 Review of the Short- and Long-Term Links between Perceptual and Cognitive Decline.
582 *Front. Aging Neurosci.* **8**, 39 (2016).
- 583 24. Eline Slagboom, P., van den Berg, N. & Deelen, J. Phenome and genome based

- 584 studies into human ageing and longevity: An overview. *Biochim. Biophys. Acta Mol.*
585 *Basis Dis.* **1864**, 2742–2751 (2018).
- 586 25. Partridge, L., Deelen, J. & Slagboom, P. E. Facing up to the global challenges of
587 ageing. *Nature* **561**, 45–56 (2018).
- 588 26. Hedden, T. & Gabrieli, J. D. E. Insights into the ageing mind: a view from cognitive
589 neuroscience. *Nat. Rev. Neurosci.* **5**, 87–96 (2004).
- 590 27. Bäckman, L., Nyberg, L., Lindenberger, U., Li, S.-C. & Farde, L. The correlative triad
591 among aging, dopamine, and cognition: current status and future prospects. *Neurosci.*
592 *Biobehav. Rev.* **30**, 791–807 (2006).
- 593 28. Solbakk, A.-K. *et al.* Altered prefrontal function with aging: insights into age-associated
594 performance decline. *Brain Res.* **1232**, 30–47 (2008).
- 595 29. Davis, S. W., Dennis, N. A., Daselaar, S. M., Fleck, M. S. & Cabeza, R. Que PASA?
596 The posterior-anterior shift in aging. *Cereb. Cortex N. Y. N 1991* **18**, 1201–1209 (2008).
- 597 30. Bishop, N. A., Lu, T. & Yankner, B. A. Neural mechanisms of ageing and cognitive
598 decline. *Nature* **464**, 529–535 (2010).
- 599 31. Grady, C. The cognitive neuroscience of ageing. *Nat. Rev. Neurosci.* **13**, 491–505
600 (2012).
- 601 32. Oswald, J. *et al.* Brain structure and cognitive ability in healthy aging: a review on
602 longitudinal correlated change. *Rev. Neurosci.* **31**, 1–57 (2019).
- 603 33. Li, H.-J. *et al.* Putting age-related task activation into large-scale brain networks: A
604 meta-analysis of 114 fMRI studies on healthy aging. *Neurosci. Biobehav. Rev.* **57**, 156–
605 174 (2015).
- 606 34. Lu, A. T. *et al.* Genetic architecture of epigenetic and neuronal ageing rates in human
607 brain regions. *Nat. Commun.* **8**, 15353 (2017).
- 608 35. Guevara, E. E. *et al.* Epigenetic ageing of the prefrontal cortex and cerebellum in
609 humans and chimpanzees. *Epigenetics* 1–12 (2022)
610 doi:10.1080/15592294.2022.2080993.
- 611 36. Proskovec, A. L. *et al.* Association of Epigenetic Metrics of Biological Age With Cortical

- 612 Thickness. *JAMA Netw. Open* **3**, e2015428 (2020).
- 613 37. Cheong, Y. *et al.* The effects of epigenetic age and its acceleration on surface area,
614 cortical thickness, and volume in young adults. *Cereb. Cortex N. Y. N* 1991 bhac043
615 (2022) doi:10.1093/cercor/bhac043.
- 616 38. Shireby, G. L. *et al.* Recalibrating the epigenetic clock: implications for assessing
617 biological age in the human cortex. *Brain J. Neurol.* **143**, 3763–3775 (2020).
- 618 39. Grodstein, F. *et al.* The association of epigenetic clocks in brain tissue with brain
619 pathologies and common aging phenotypes. *Neurobiol. Dis.* **157**, 105428 (2021).
- 620 40. Aa, D. *et al.* Transcriptomic profiling of the human brain reveals that altered synaptic
621 gene expression is associated with chronological aging. *Sci. Rep.* **7**, (2017).
- 622 41. French, L., Ma, T., Oh, H., Tseng, G. C. & Sibille, E. Age-Related Gene Expression in
623 the Frontal Cortex Suggests Synaptic Function Changes in Specific Inhibitory Neuron
624 Subtypes. *Front. Aging Neurosci.* **9**, 162 (2017).
- 625 42. Hu, Y. *et al.* Gene Expression Analysis Reveals Novel Gene Signatures Between
626 Young and Old Adults in Human Prefrontal Cortex. *Front. Aging Neurosci.* **10**, 259
627 (2018).
- 628 43. Wruck, W. & Adjaye, J. Meta-analysis of human prefrontal cortex reveals activation of
629 GFAP and decline of synaptic transmission in the aging brain. *Acta Neuropathol.*
630 *Commun.* **8**, 26 (2020).
- 631 44. Zhao, X. *et al.* PTSD, major depression, and advanced transcriptomic age in brain
632 tissue. *Depress. Anxiety* (2022) doi:10.1002/da.23289.
- 633 45. Liberzon, A. *et al.* The Molecular Signatures Database (MSigDB) hallmark gene set
634 collection. *Cell Syst.* **1**, 417–425 (2015).
- 635 46. de Magalhães, J. P., Costa, J. & Toussaint, O. HAGR: the Human Ageing Genomic
636 Resources. *Nucleic Acids Res.* **33**, D537-543 (2005).
- 637 47. Galkin, F., Mamoshina, P., Kochetov, K., Sidorenko, D. & Zhavoronkov, A. DeepMAge:
638 A Methylation Aging Clock Developed with Deep Learning. *Aging Dis.* **12**, 1252–1262
639 (2021).

- 640 48. de Lima Camillo, L. P., Lapierre, L. R. & Singh, R. A pan-tissue DNA-methylation
641 epigenetic clock based on deep learning. *npj Aging* vol. 8 (2022).
- 642 49. Galkin, F. *et al.* Biohorology and biomarkers of aging: Current state-of-the-art,
643 challenges and opportunities. *Ageing Res. Rev.* **60**, 101050 (2020).
- 644 50. Kuan, P.-F. *et al.* PTSD is associated with accelerated transcriptional aging in World
645 Trade Center responders. *Transl. Psychiatry* **11**, 311 (2021).
- 646 51. Wolf, E. J. *et al.* Klotho, PTSD, and advanced epigenetic age in cortical tissue.
647 *Neuropsychopharmacol. Off. Publ. Am. Coll. Neuropsychopharmacol.* **46**, 721–730
648 (2021).
- 649 52. Snir, S., Farrell, C. & Pellegrini, M. Human epigenetic ageing is logarithmic with time
650 across the entire lifespan. *Epigenetics* **14**, 912–926 (2019).
- 651 53. Nevalainen, T. *et al.* Obesity accelerates epigenetic aging in middle-aged but not in
652 elderly individuals. *Clin. Epigenetics* **9**, 20 (2017).
- 653 54. Sugo, S. *et al.* Endothelial cells actively synthesize and secrete adrenomedullin.
654 *Biochem. Biophys. Res. Commun.* **201**, 1160–1166 (1994).
- 655 55. Kis, B., Chen, L., Ueta, Y. & Busija, D. W. Autocrine peptide mediators of cerebral
656 endothelial cells and their role in the regulation of blood-brain barrier. *Peptides* **27**,
657 211–222 (2006).
- 658 56. Larrayoz, I. M. *et al.* Adrenomedullin Contributes to Age-Related Memory Loss in Mice
659 and Is Elevated in Aging Human Brains. *Front. Mol. Neurosci.* **10**, 384 (2017).
- 660 57. Mitome-Mishima, Y. *et al.* Adrenomedullin deficiency and aging exacerbate ischemic
661 white matter injury after prolonged cerebral hypoperfusion in mice. *BioMed Res. Int.*
662 **2014**, 861632 (2014).
- 663 58. Iram, T. *et al.* Young CSF restores oligodendrogenesis and memory in aged mice via
664 Fgf17. *Nature* **605**, 509–515 (2022).
- 665 59. Morrison, J. H. & Baxter, M. G. The ageing cortical synapse: hallmarks and implications
666 for cognitive decline. *Nat. Rev. Neurosci.* **13**, 240–250 (2012).
- 667 60. Johri, A. & Beal, M. F. Mitochondrial dysfunction in neurodegenerative diseases. *J.*

- 668 *Pharmacol. Exp. Ther.* **342**, 619–630 (2012).
- 669 61. Kr, S. *et al.* Presynaptic dystrophic neurites surrounding amyloid plaques are sites of
670 microtubule disruption, BACE1 elevation, and increased A β generation in Alzheimer's
671 disease. *Acta Neuropathol. (Berl.)* **132**, (2016).
- 672 62. Bhatia, V. & Sharma, S. Role of mitochondrial dysfunction, oxidative stress and
673 autophagy in progression of Alzheimer's disease. *J. Neurol. Sci.* **421**, 117253 (2021).
- 674 63. Misrani, A., Tabassum, S. & Yang, L. Mitochondrial Dysfunction and Oxidative Stress in
675 Alzheimer's Disease. *Front. Aging Neurosci.* **13**, 617588 (2021).
- 676 64. Kopeikina, K. J. *et al.* Tau Accumulation Causes Mitochondrial Distribution Deficits in
677 Neurons in a Mouse Model of Tauopathy and in Human Alzheimer's Disease Brain.
678 *Am. J. Pathol.* **179**, 2071–2082 (2011).
- 679 65. Atamna, H. & Frey, W. H. Mechanisms of mitochondrial dysfunction and energy
680 deficiency in Alzheimer's disease. *Mitochondrion* **7**, 297–310 (2007).
- 681 66. Calvo-Rodriguez, M. *et al.* Increased mitochondrial calcium levels associated with
682 neuronal death in a mouse model of Alzheimer's disease. *Nat. Commun.* **11**, 2146
683 (2020).
- 684 67. Bruns, D. R. *et al.* Nrf2 Signaling and the Slowed Aging Phenotype: Evidence from
685 Long-Lived Models. *Oxid. Med. Cell. Longev.* **2015**, 732596 (2015).
- 686 68. Kobayashi, M. & Yamamoto, M. Nrf2-Keap1 regulation of cellular defense mechanisms
687 against electrophiles and reactive oxygen species. *Adv. Enzyme Regul.* **46**, 113–140
688 (2006).
- 689 69. Jain, A. *et al.* p62/SQSTM1 is a target gene for transcription factor NRF2 and creates a
690 positive feedback loop by inducing antioxidant response element-driven gene
691 transcription. *J. Biol. Chem.* **285**, 22576–22591 (2010).
- 692 70. Kim, J., Cha, Y.-N. & Surh, Y.-J. A protective role of nuclear factor-erythroid 2-related
693 factor-2 (Nrf2) in inflammatory disorders. *Mutat. Res.* **690**, 12–23 (2010).
- 694 71. Pickering, A. M., Linder, R. A., Zhang, H., Forman, H. J. & Davies, K. J. A. Nrf2-
695 dependent induction of proteasome and Pa28 $\alpha\beta$ regulator are required for adaptation


- 696 to oxidative stress. *J. Biol. Chem.* **287**, 10021–10031 (2012).
- 697 72. Lewis, K. N., Mele, J., Hornsby, P. J. & Buffenstein, R. Stress resistance in the naked
698 mole-rat: the bare essentials - a mini-review. *Gerontology* **58**, 453–462 (2012).
- 699 73. Lewis, K. N. *et al.* Regulation of Nrf2 signaling and longevity in naturally long-lived
700 rodents. *Proc. Natl. Acad. Sci. U. S. A.* **112**, 3722–3727 (2015).
- 701 74. Chen, L. H., Hu, N. & Snyder, D. L. Effects of age and dietary restriction on liver
702 glutathione transferase activities in Lobund-Wistar rats. *Arch. Gerontol. Geriatr.* **18**,
703 191–205 (1994).
- 704 75. Balogun, E. *et al.* Curcumin activates the haem oxygenase-1 gene via regulation of
705 Nrf2 and the antioxidant-responsive element. *Biochem. J.* **371**, 887–895 (2003).
- 706 76. Chen, C.-Y., Jang, J.-H., Li, M.-H. & Surh, Y.-J. Resveratrol upregulates heme
707 oxygenase-1 expression via activation of NF-E2-related factor 2 in PC12 cells.
708 *Biochem. Biophys. Res. Commun.* **331**, 993–1000 (2005).
- 709 77. Hyun, D.-H., Emerson, S. S., Jo, D.-G., Mattson, M. P. & de Cabo, R. Calorie restriction
710 up-regulates the plasma membrane redox system in brain cells and suppresses
711 oxidative stress during aging. *Proc. Natl. Acad. Sci. U. S. A.* **103**, 19908–19912 (2006).
- 712 78. Csiszar, A. *et al.* Caloric restriction confers persistent anti-oxidative, pro-angiogenic,
713 and anti-inflammatory effects and promotes anti-aging miRNA expression profile in
714 cerebrovascular endothelial cells of aged rats. *Am. J. Physiol. Heart Circ. Physiol.*
715 **307**, H292-306 (2014).
- 716 79. Girgenti, M. J. *et al.* Transcriptomic organization of the human brain in post-traumatic
717 stress disorder. *Nat. Neurosci.* **24**, 24–33 (2021).
- 718 80. Friedman, M. J. *et al.* VA's National PTSD Brain Bank: a National Resource for
719 Research. *Curr. Psychiatry Rep.* **19**, 73 (2017).
- 720 81. Dobin, A. *et al.* STAR: ultrafast universal RNA-seq aligner. *Bioinforma. Oxf. Engl.* **29**,
721 15–21 (2013).
- 722 82. Graubert, A., Aguet, F., Ravi, A., Ardlie, K. G. & Getz, G. RNA-SeQC 2: Efficient RNA-
723 seq quality control and quantification for large cohorts. *Bioinforma. Oxf. Engl.* btab135

- 724 (2021) doi:10.1093/bioinformatics/btab135.
- 725 83. Hansen, K. D., Irizarry, R. A. & Wu, Z. Removing technical variability in RNA-seq data
726 using conditional quantile normalization. *Biostat. Oxf. Engl.* **13**, 204–216 (2012).
- 727 84. R Core Team. *R: A language and environment for statistical computing*. (R Foundation
728 for Statistical Computing, 2020).
- 729 85. McKenzie, A. T. *et al.* Brain Cell Type Specific Gene Expression and Co-expression
730 Network Architectures. *Sci. Rep.* **8**, 8868 (2018).
- 731 86. Skene, N. G. & Grant, S. G. N. Identification of Vulnerable Cell Types in Major Brain
732 Disorders Using Single Cell Transcriptomes and Expression Weighted Cell Type
733 Enrichment. *Front. Neurosci.* **10**, 16 (2016).
- 734 87. Barabási, A.-L. & Oltvai, Z. N. Network biology: understanding the cell's functional
735 organization. *Nat. Rev. Genet.* **5**, 101–113 (2004).
- 736 88. Furlong, L. I. Human diseases through the lens of network biology. *Trends Genet. TIG*
737 **29**, 150–159 (2013).
- 738 89. Arshad, Z. & McDonald, J. F. A computational approach to generate highly conserved
739 gene co-expression networks with RNA-seq data. *STAR Protoc.* **3**, 101432 (2022).
- 740 90. Morselli Gysi, D. *et al.* Whole transcriptomic network analysis using Co-expression
741 Differential Network Analysis (CoDiNA). *PLoS One* **15**, e0240523 (2020).
- 742 91. Gysi, D. M., Voigt, A., Fragoso, T. de M., Almaas, E. & Nowick, K. wTO: an R package
743 for computing weighted topological overlap and a consensus network with integrated
744 visualization tool. *BMC Bioinformatics* **19**, 392 (2018).
- 745 92. Zhou, Y. *et al.* Metascape provides a biologist-oriented resource for the analysis of
746 systems-level datasets. *Nat. Commun.* **10**, 1523 (2019).
- 747 93. Bader, G. D. & Hogue, C. W. V. An automated method for finding molecular complexes
748 in large protein interaction networks. *BMC Bioinformatics* **4**, 2 (2003).
- 749 94. Koopmans, F. *et al.* SynGO: An Evidence-Based, Expert-Curated Knowledge Base for
750 the Synapse. *Neuron* **103**, 217-234.e4 (2019).
- 751

752

753

754


Postmortem Human Prefrontal Cortex Biopsies
(n = 551 samples)


RNASeq

Transcriptomic clocks

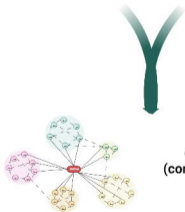


Deep neural clock
(Holzscheck et al. 2021)

- Variable number of genes
- Learn from the data

RNAAgeCalc
(Ren & Kuan 2020)

- Fixed number of genes



**Co-expression
(consensus networks)**

Phenotypic correlations



- Age prediction accuracy
- Age - squared analysis
- Phenotypic traits

Disease risk

Functional analysis



Pathway Enrichment

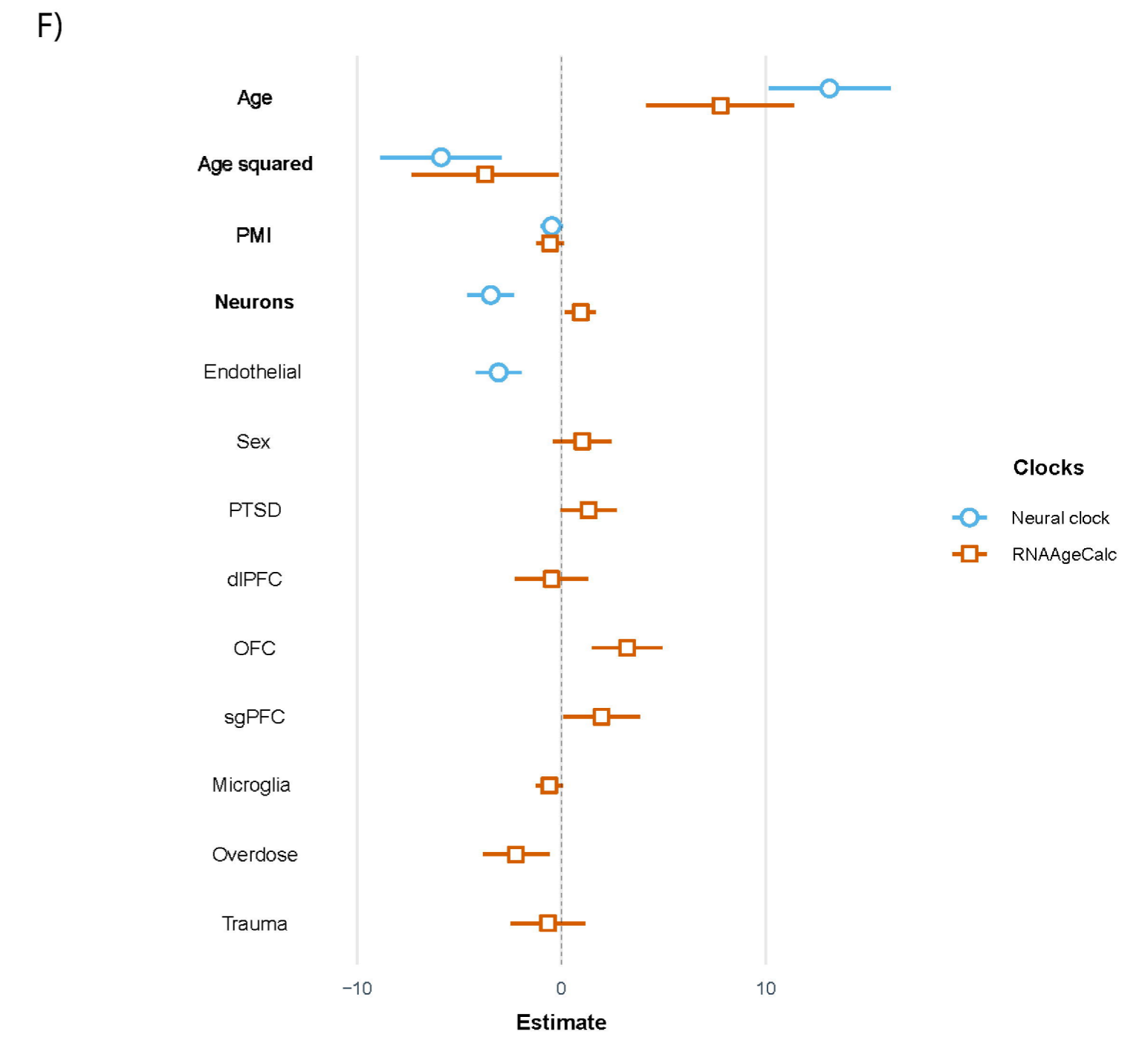
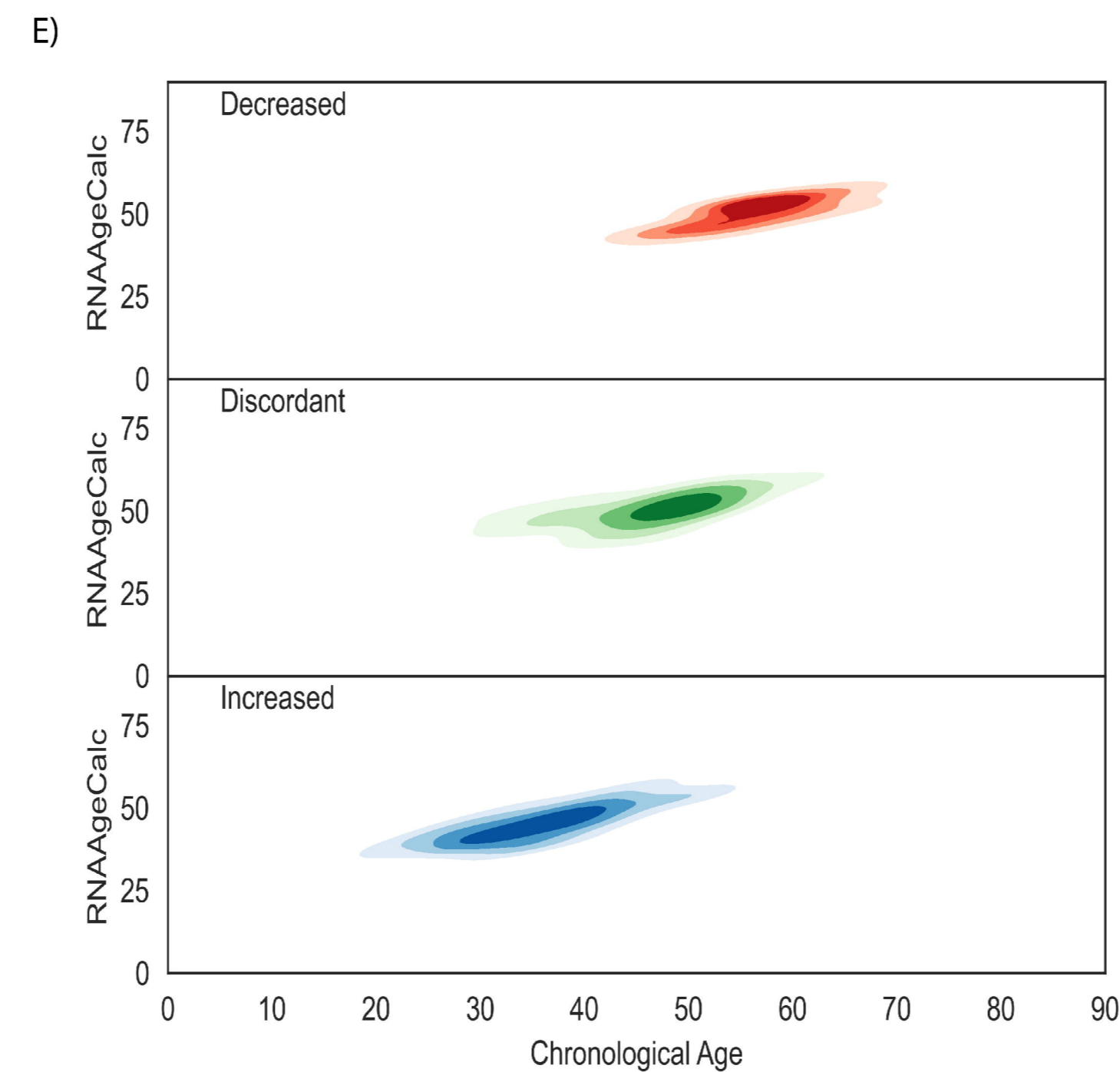
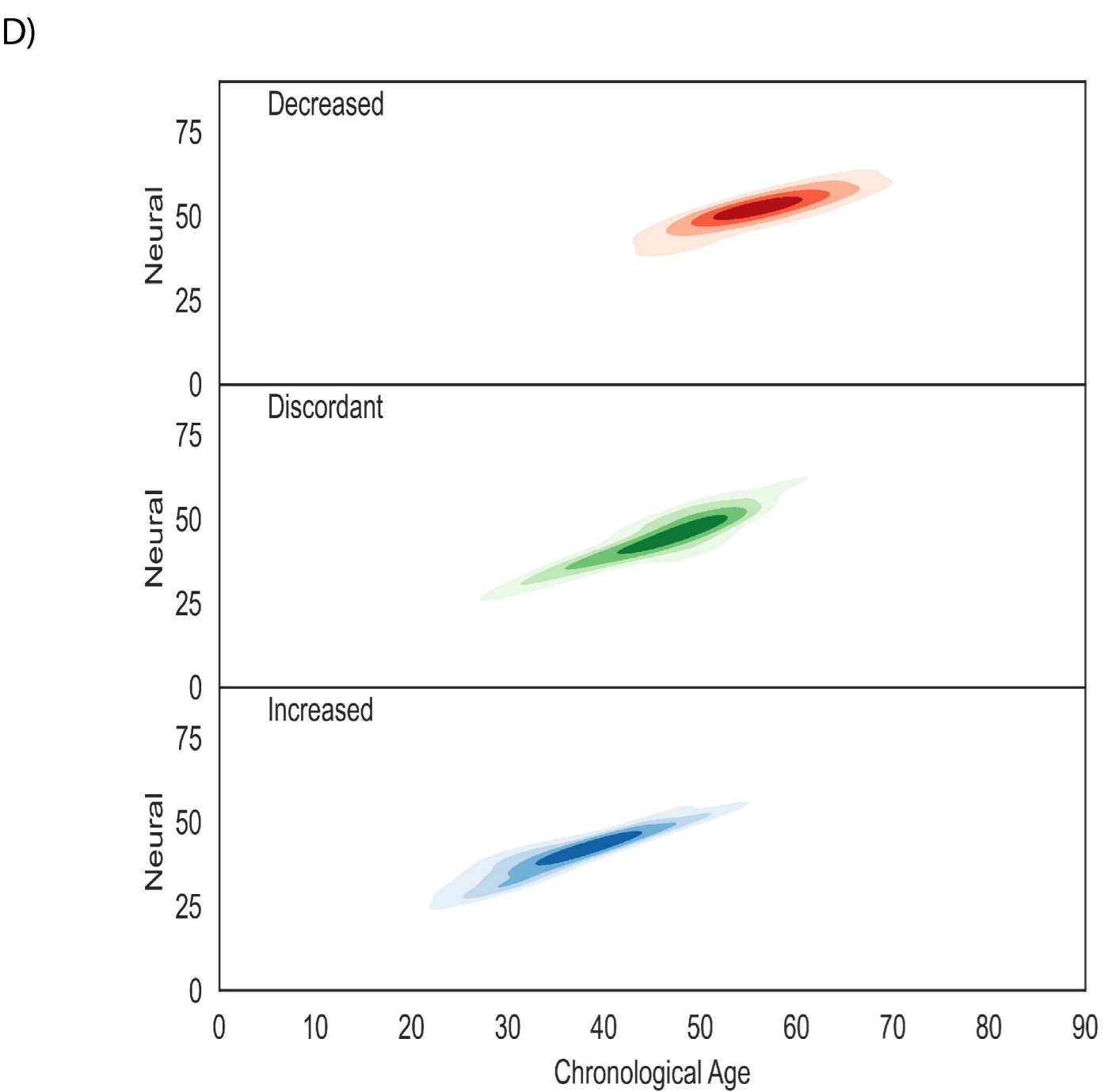
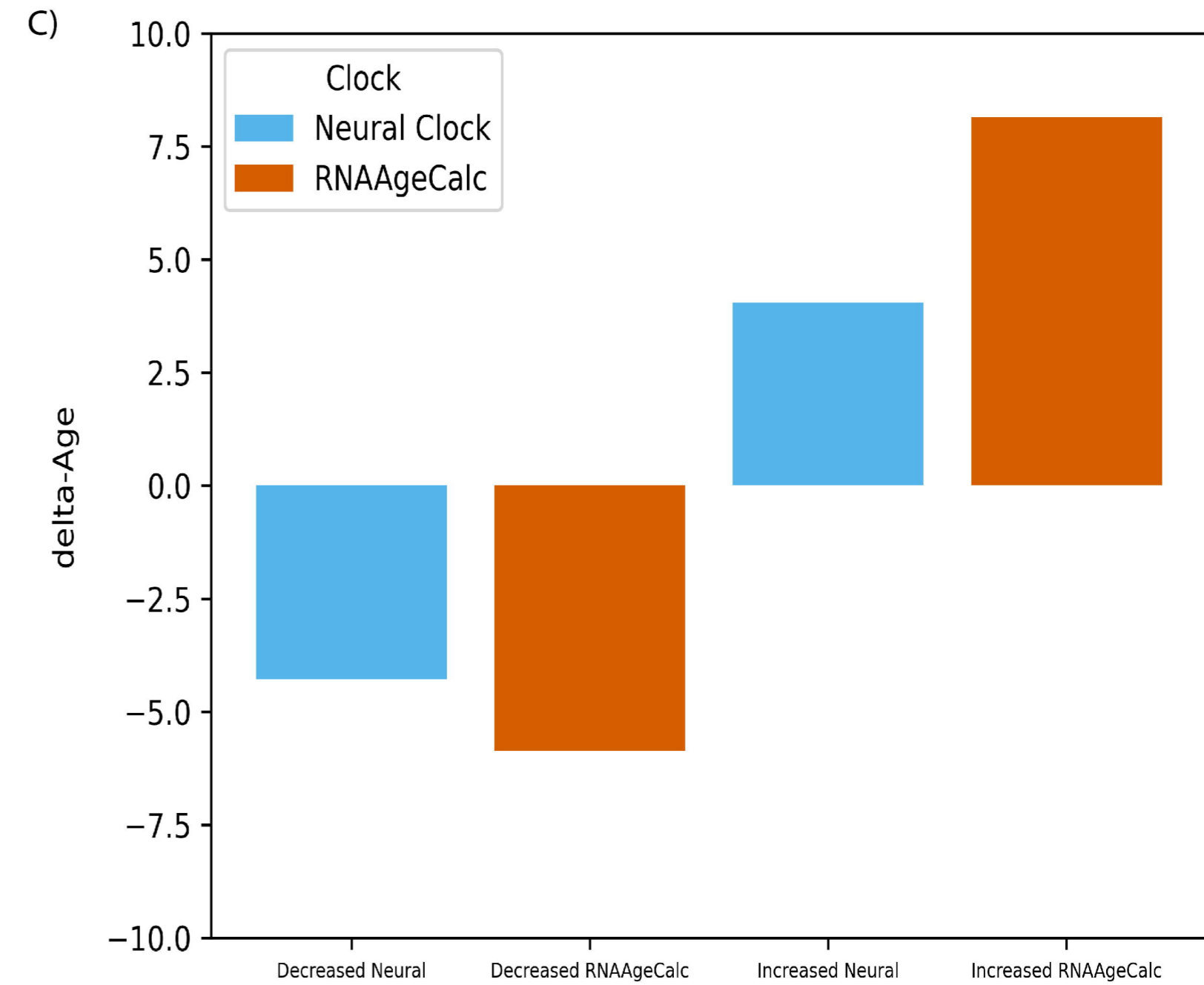
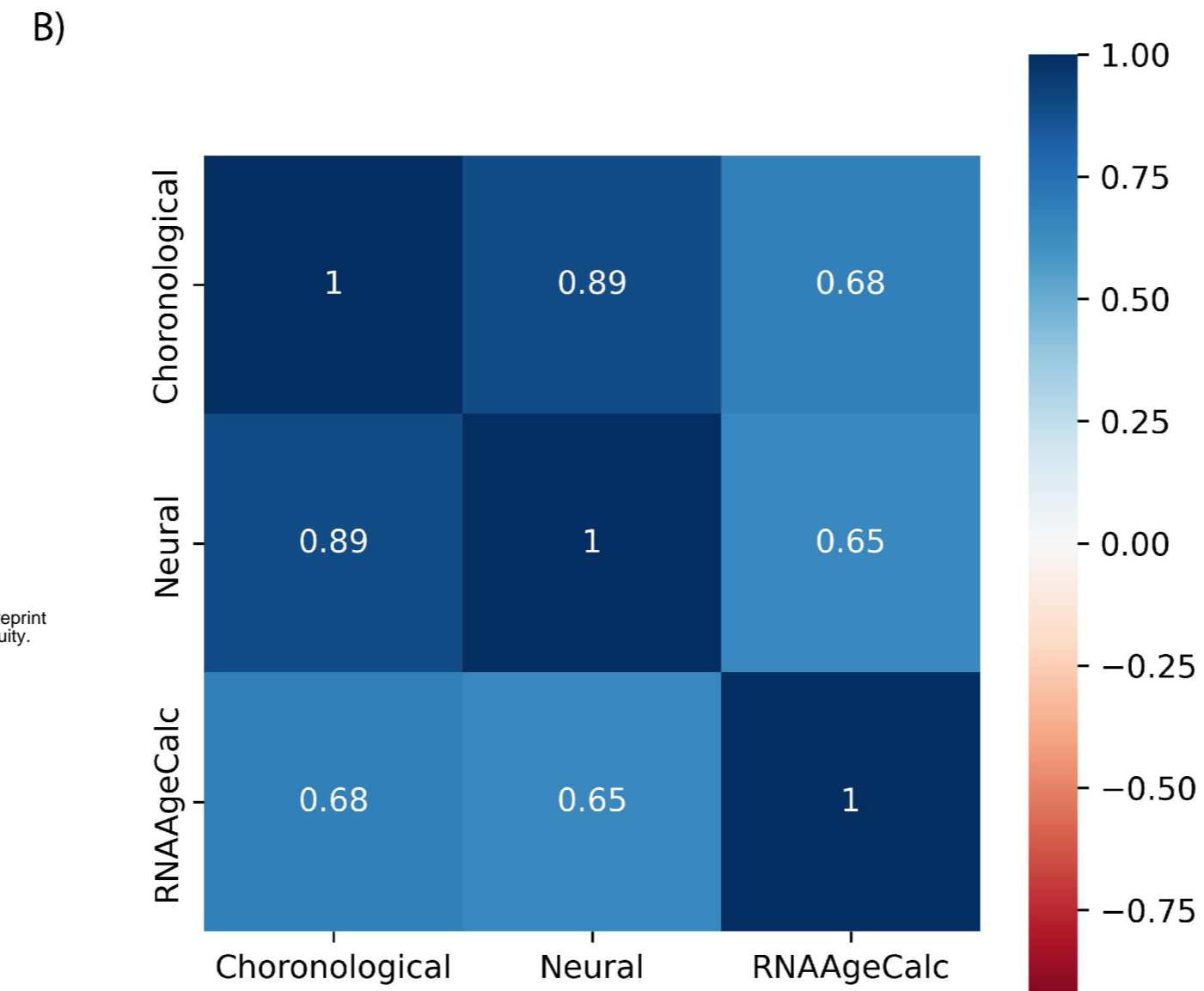
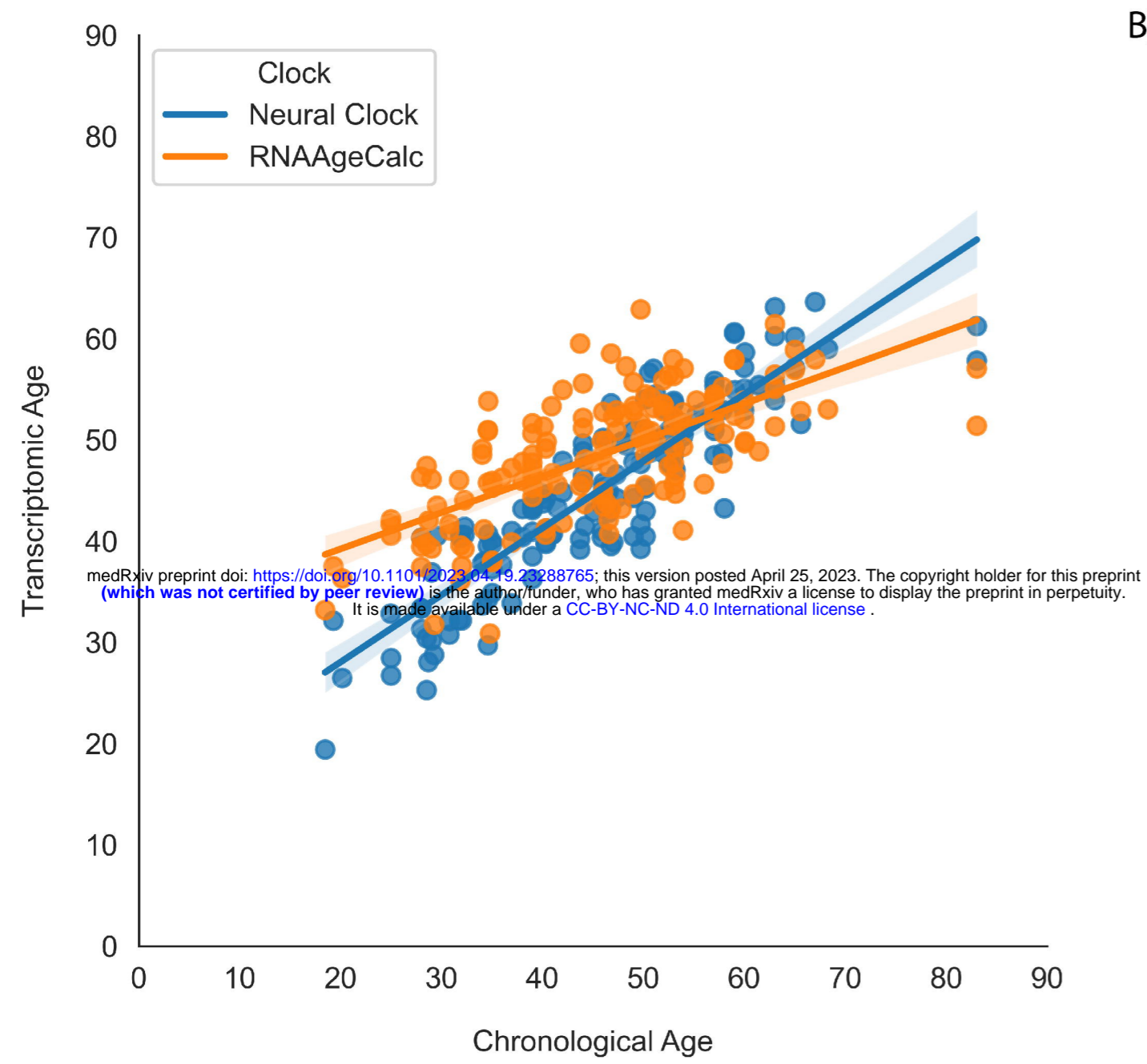
FUMAGWAS

Genome-wide Association
Enrichment

Functional impact



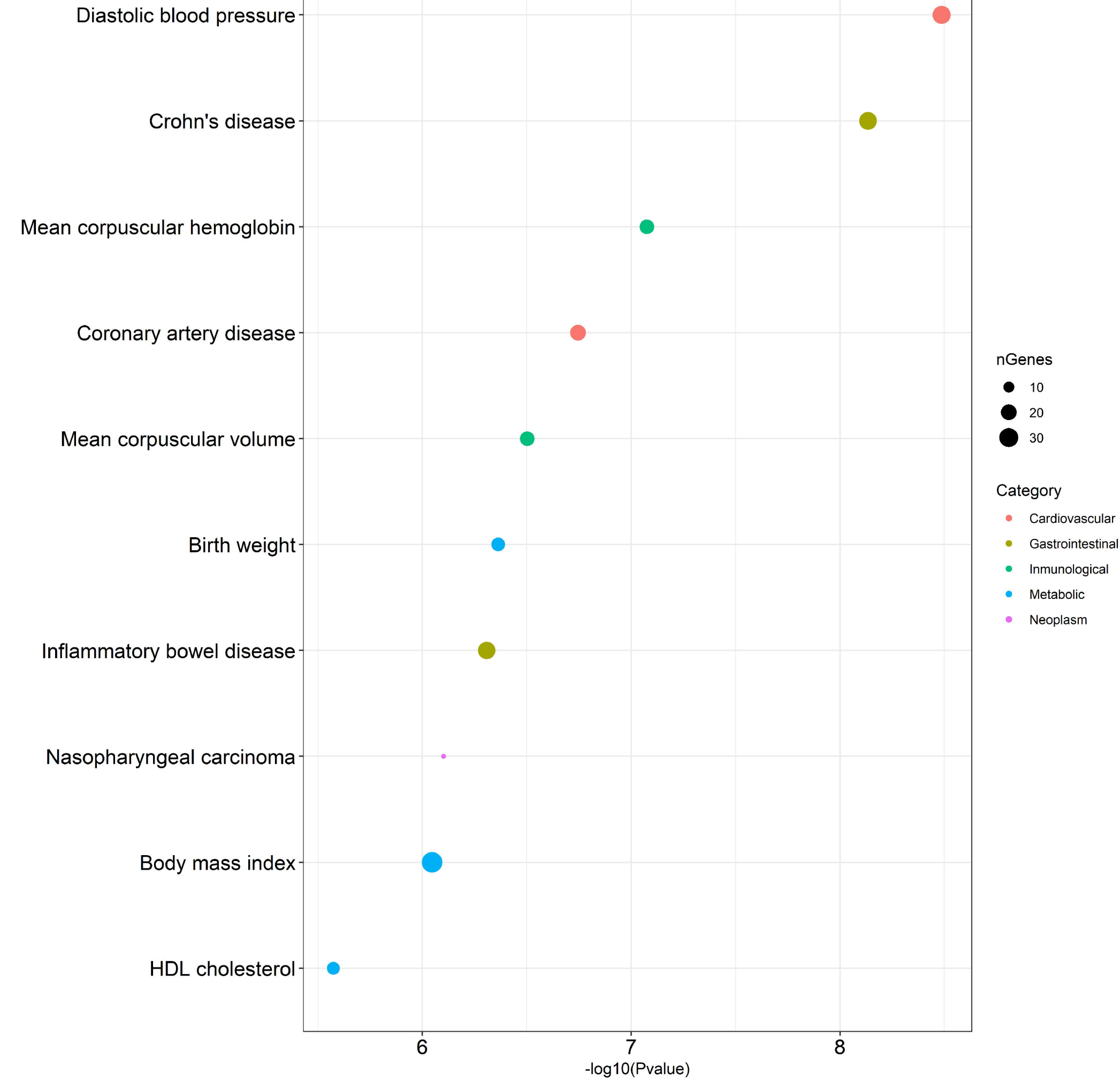
Synaptic Enrichment



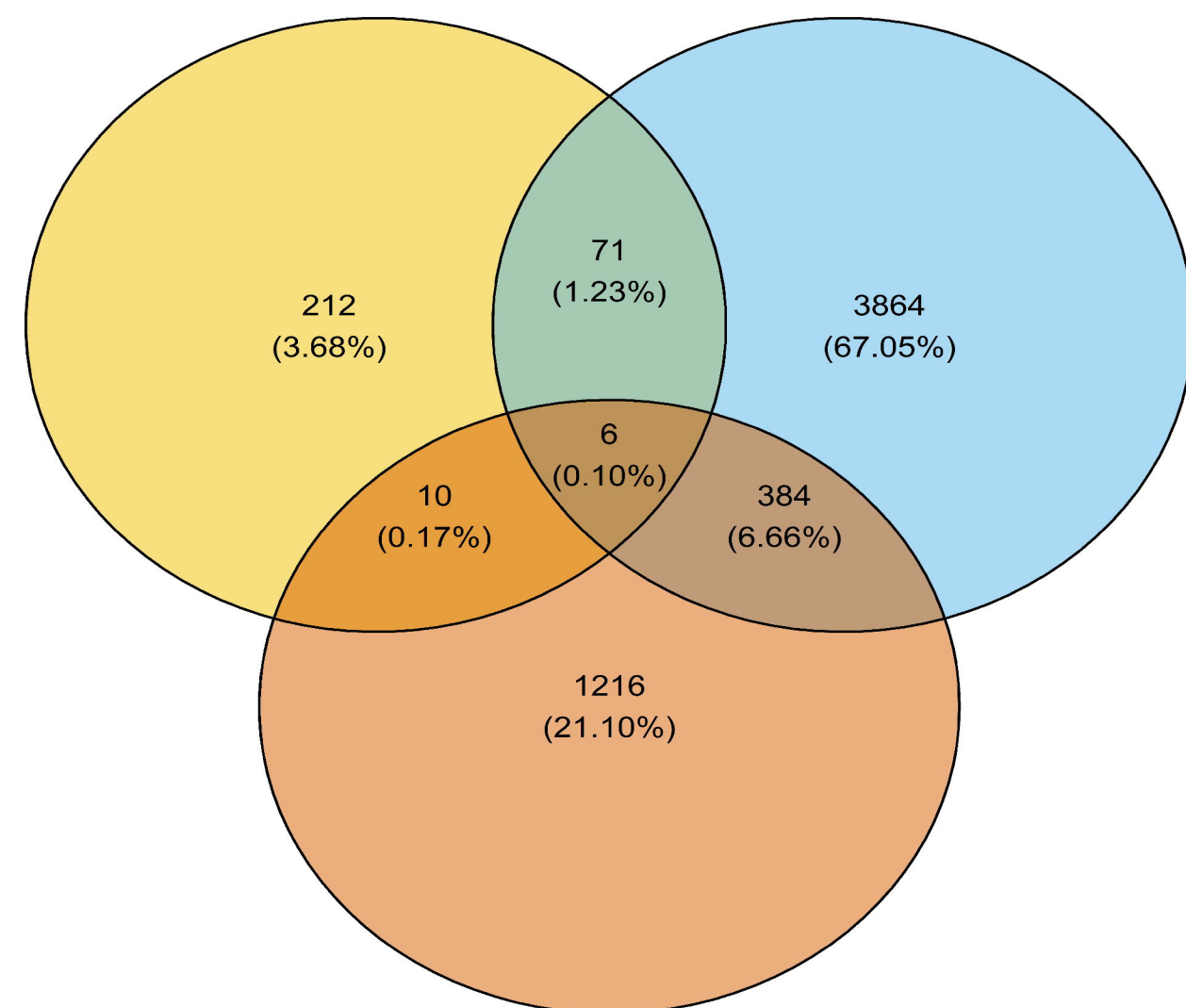
A)



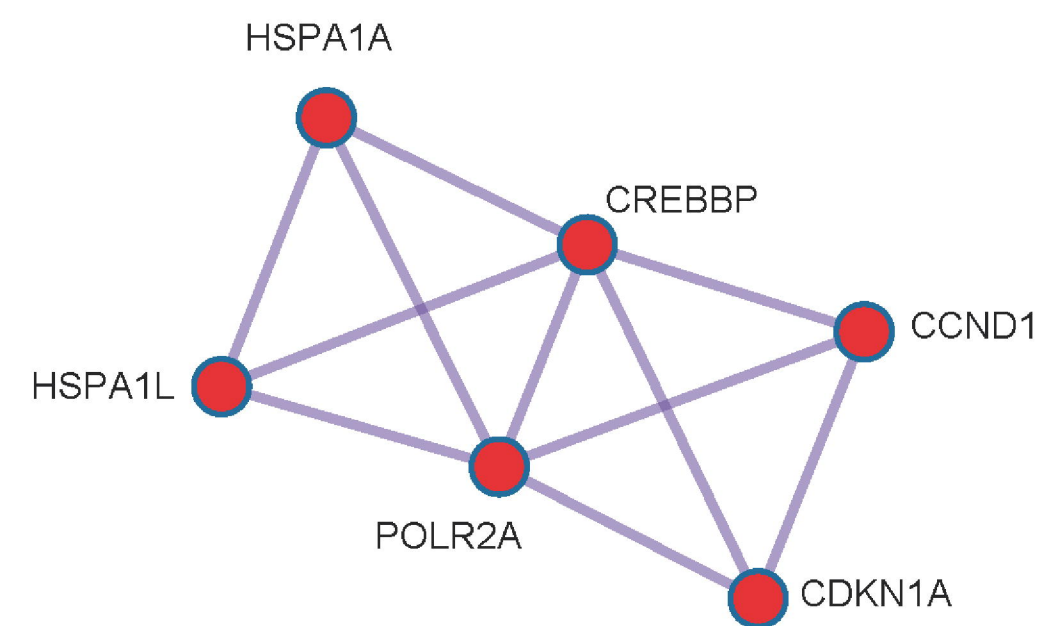
B)



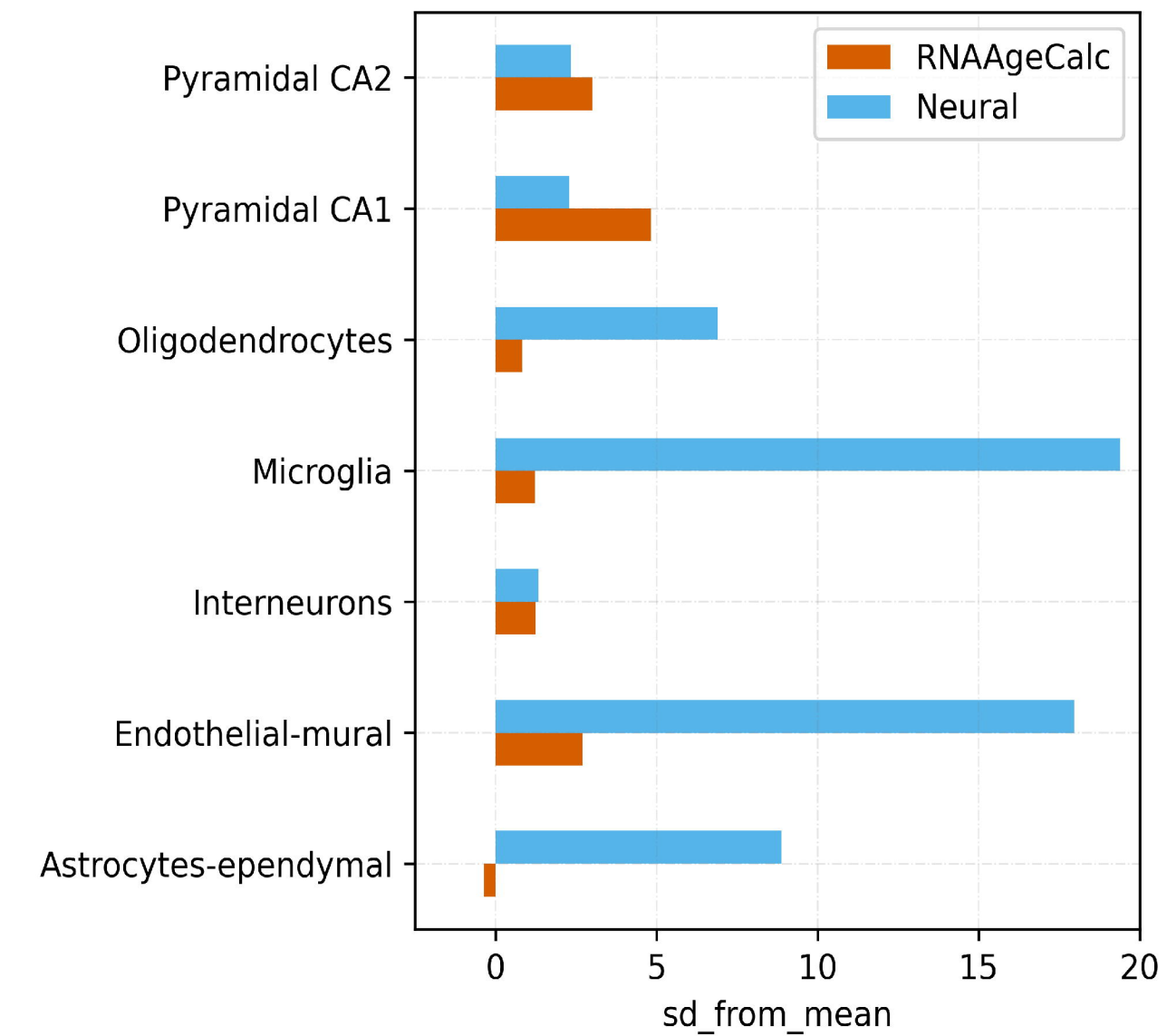
C)



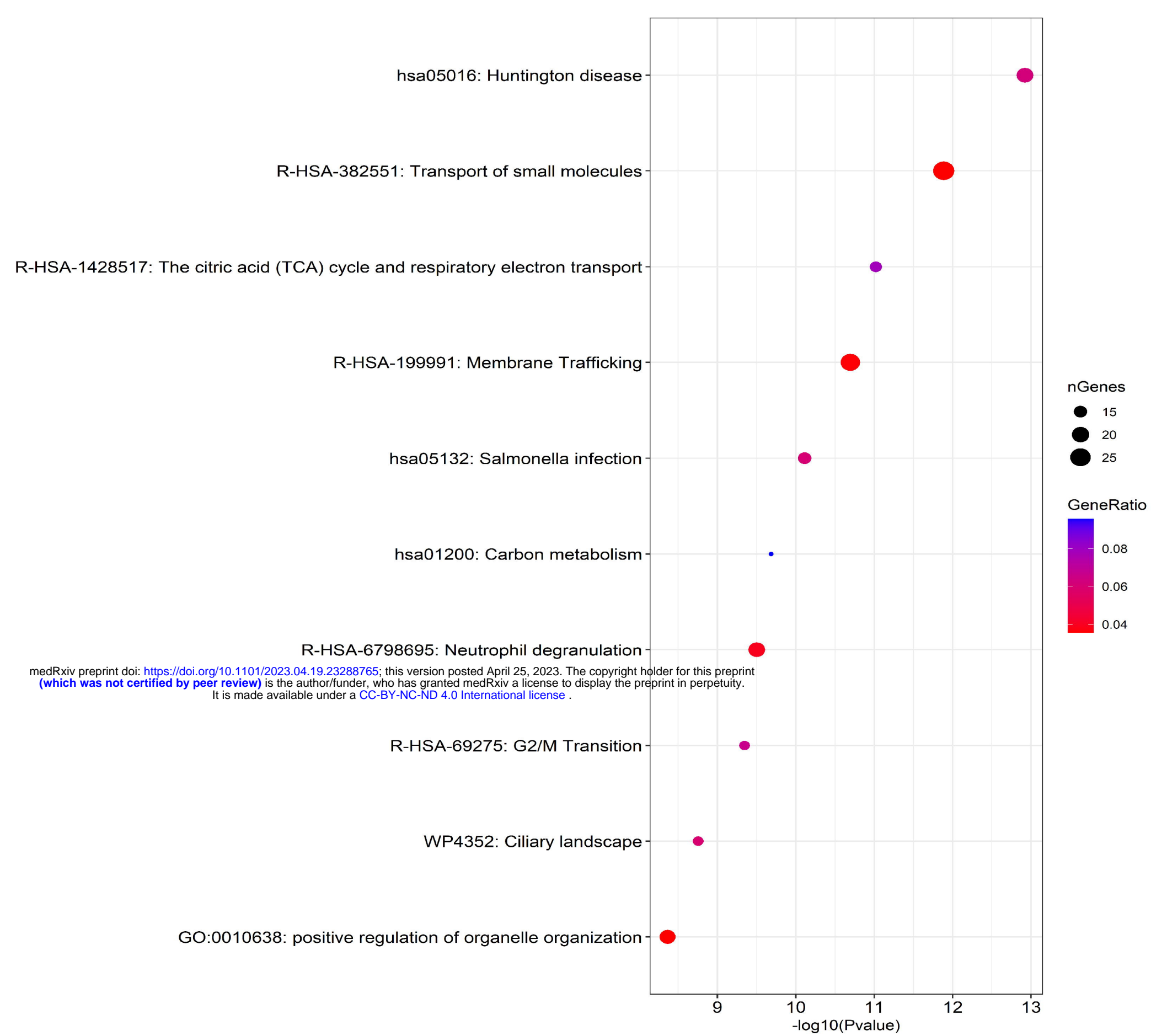
D)



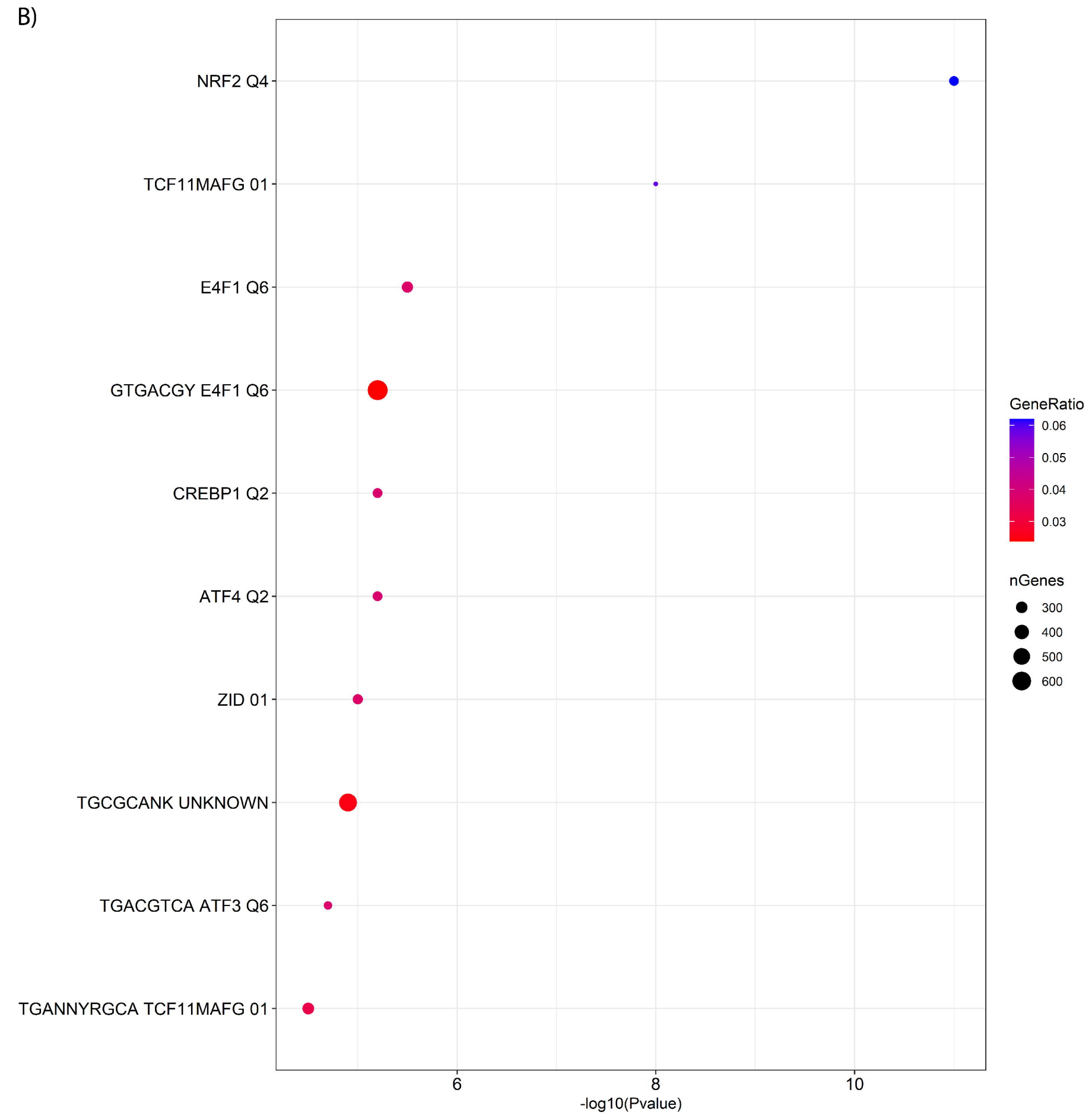
E)



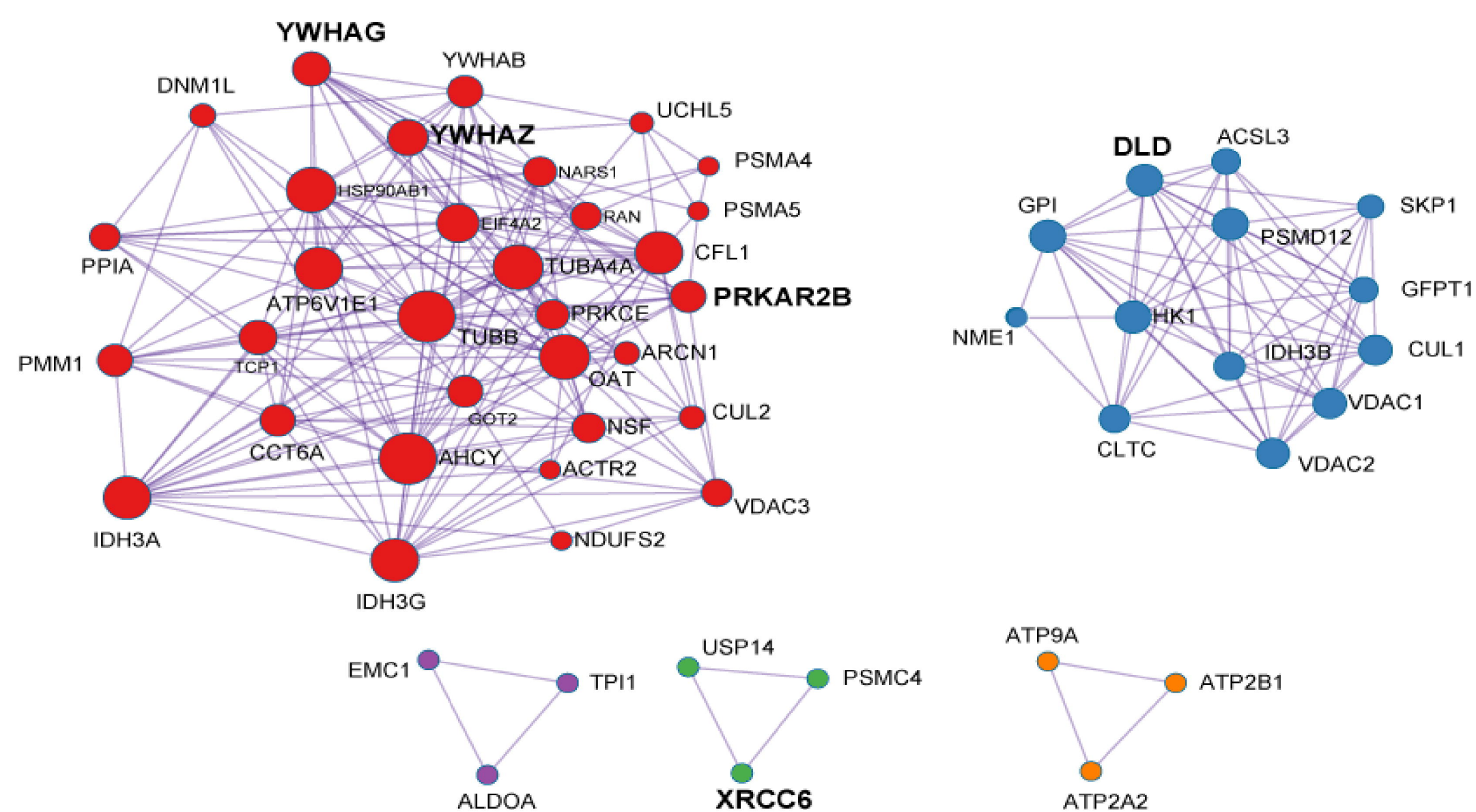
A)



B)



C)



D)

